ture variations of up to several hundred degrees.

The center frequency f_c of each spectrum was estimated as that frequency which splits the received power into equal halves; that is

$$\int_0^{f_c} S(f)df = \int_{f_c}^{100} S(f)df$$

The bandwidth B of each spectrum was estimated, similarly, as that band which contains the central half of the signal power

$$\int_0^{f_1} S(f)df = 1/4\, P_s$$

$$\int_{f_2}^{100} S(f)df = 3/4\, P_s$$

$$B = f_2 - f_1$$

Figure 3 is a sequence of spectrograms taken on 8 November when Pioneer 6 was 2.4 degrees away from the sun and approaching the sun. This figure shows the effect of increased turbulence in the corona, presumably caused by some solar "event." The effects lasted several hours, the decay being much slower than the onset. Only six such events were observed. Most of the spectra were constant, showing only a slow thermal drift of the spacecraft frequency.

The results of the experiment are summarized in Fig. 4, where the bandwidth and power of each spectrum are plotted against the date. The average center frequency for each day is also plotted.

Two separate phenomena are manifested in Fig. 4. The first is the occasional marked increase in bandwidth caused by the solar events mentioned above. The second is a background bandwidth of about 1 hz, due to frequency instabilities of the system, which appeared when Pioneer 6 was far from the sun. This component increased slowly as the rays penetrated more deeply into the corona. Finally, the bandwidth increased very rapidly at about 1 degree from the sun, just before the signal disappeared. The effect is as though the solar radius were 1 degree at S-band.

The measurements of power do not seem to correlate with those of bandwidth. In particular, the power fluctuations do not correspond to the sudden increases in bandwidth induced by the solar events. Although there is considerable scatter associated with the power estimates, they are on the whole relatively constant throughout the experiment. The only exception would be the 2 days at 1 degree when the power appears to be somewhat smaller.

The nature of the solar events is not known. They do not appear to correlate well with solar flares or with the apparition of sunspots on the solar limb or with the S-band solar flux. They may be the result of streamers sweeping across the line of sight.

In the hope of establishing a correlation of the spectral broadening with other solar phenomena, I present in Table 1 the times and durations of the observed events. Table 1 also gives the times when spectrograms were taken but no events were observed. A full set of spectrograms will soon be available (*2*).

R. M. GOLDSTEIN
Jet Propulsion Laboratory, California Institute of Technology, Pasadena

References and Notes

1. G. S. Levy, T. Sato, B. L. Seidel, C. T. Stelzried, J. E. Ohlson, W. V. T. Rusch, *Science*, this issue.
2. R. M. Goldstein, *Jet Propulsion Lab. Tech. Rep. TR 32–1435* (1969).
3. This paper presents the results of one phase of research carried out at the Jet Propulsion Laboratory, California Institute of Technology, under NASA contract No. NAS 7-100.

24 June 1969

Seismic Activity and Faulting Associated with a Large Underground Nuclear Explosion

Abstract. *The 1.1-megaton nuclear test Benham caused movement on previously mapped faults and was followed by a sequence of small earthquakes. These effects were confined to a zone extending not more than 13 kilometers from ground zero; they are apparently related to the release of natural tectonic strain.*

On 19 December 1968, a 1.1-megaton nuclear explosion was detonated 1.4 km beneath Pahute Mesa at the Nevada Test Site. This explosion, code named Benham, caused movement on nearby faults and was followed by a sequence of earthquakes lasting several months. Such phenomena have been observed for earlier explosions, but this was the first test that was monitored by a dense network of seismograph stations capable of locating the aftershocks with high accuracy and defining the *P*-wave first-motion pattern in sufficient detail to determine the earthquake mechanism.

Movements along faults or fractures are observed near most underground tests. When these effects were first observed, it was thought that they were probably related either to deformations caused by the formation of the underground cavity or to compaction of the rocks in the vicinity of the test. As the number and size of tests increased, however, it became apparent that these explanations were inadequate. Displacements as great as 1 m along virtually continuous fractures extending for distances of as much as 8.5 km were observed at both Yucca Flat and Pahute Mesa in southern Nevada, and Hot Creek Valley in central Nevada. Such movement was not entirely unexpected; it was in fact anticipated for the Aardvark event and reported (*1*). Many subsequent occurrences of fault movement have been reported (*2, 3*). Since 1966, a number of nuclear tests have caused fault movement in bedrock that could not be explained by differential compaction of poorly consolidated alluvium. On those faults where the direction of previous vertical movement could be determined, the movement caused by the explosion was always in the same direction as the last recognizable tectonic movement.

The first reports of seismic activity following underground nuclear explosions were made by Westphal (*4*), who described the intense seismicity near the detonation point and concluded that most of the earthquakes were associated with the collapse of the cavity formed by the explosion. A few earthquakes, however, were located too far from the cavity to be associated with the collapse phenomena.

A number of investigators studying the radiation pattern of seismic waves have reported that their observations could not be explained by a simple explosive source in a homogeneous medium. Press and Archambeau (*5*) reported a strong excitation of horizontally polarized shear waves (*SH* waves) and examined the possibility that these waves might result from insertion of a spherical cavity in a strained medium. They concluded that a cavity the size of the crushed zone would not release sufficient tectonic energy to produce the observed amplitudes. Brune and Pomeroy (*6*), on the basis of observation of a surface-wave radiation pattern with a double-couple symmetry, reported that the Hardhat explosion had triggered release of tectonic strain. They concluded that movement along fault planes extending beyond the

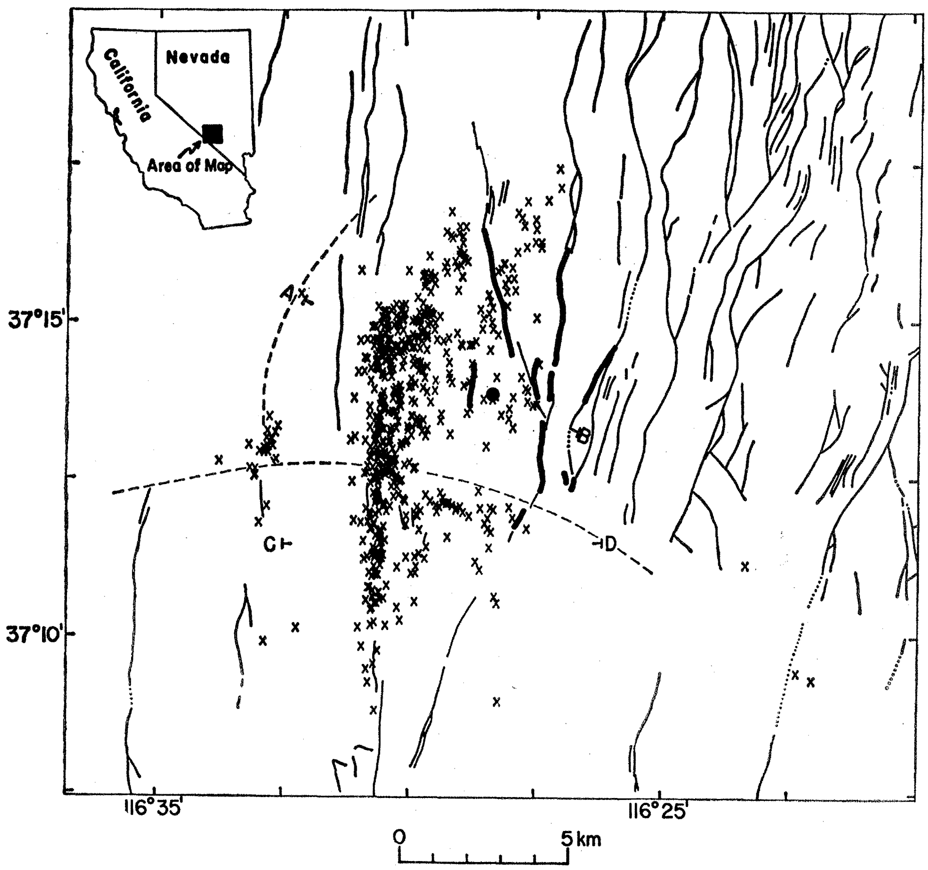

Fig. 1. Epicenters and faults. Thin lines denote faults mapped prior to the Benham event; thick lines, faults that moved during or shortly after the Benham event. Crosses, epicenter; solid circle, the Benham site; *AB* and *CD* are the lines of the vertical sections in Fig. 2.

radius of the cavity would be required to produce the observed amplitudes. Radiation patterns from the Hardhat, Haymaker, and Shoal explosions, analyzed by Toksöz and his co-workers (*7*), also indicated the release of tectonic strain. These workers concluded that the radiation pattern from Hardhat could not be explained by strain release from a rock volume the size of the crushed zone and suggested that "An earthquake, triggered . . . near the explosion, would be an explanation . . . of the observed strain energy."

In 1968, Ryall and his colleagues reported that many of the seismic events following nuclear tests were located at a considerable distance from ground zero. Boucher, Ryall, and Jones (*8*) studied a number of nuclear detonations and reported that all explosions with a seismic body-wave magnitude greater than 5.0 were followed by an increase in seismicity within 20 km of ground zero. In one case, the Faultless test in central Nevada, a zone 40 km from ground zero, was active following the test. Evernden (*9*) determined the magnitude of nuclear events and their associated earthquakes and found that all of the earthquakes following a test are at least 2 units of magnitude smaller than the explosion.

Ryall and Savage (*10*) investigated the Boxcar event of 26 April 1968, with a small tripartite array located 14 km from ground zero. They found a northeast-trending epicentral region 12 km long and 3 to 4 km wide, centered approximately on ground zero; focal depths were thought to be as great as 6 km. The major faulting observed by Dickey and co-workers at the surface following this event was along northerly-trending faults (*2*) and was not clearly related to the earthquake pattern.

Because of these reports, a seismograph network including 27 stations within 32 km of ground zero was established by the U.S. Geological Survey to study the Benham event. Observations began 12 days before the shot and have continued to the present time.

In the 12 days preceding the Benham detonation, only three earthquakes with body-wave magnitude greater than 1.3 were detected. Following the detonation, seismic activity commenced at a high rate. During the first day, more than 1000 events with magnitude greater than 1.3 were observed. The rate dropped steadily to about 15 events per day on day 15 after the test, and then increased again to a level of about 140 per day on day 24. Following this second peak, there was an uninterrupted decline to a level of five events per day on day 40. Occasional earthquakes were still observed several months after the test, but it is difficult to determine if these events are associated with the Benham test.

Two types of seismic events were observed. One was characterized by a sharp beginning and a variation in radiation pattern with azimuth from the event. The other was characterized by a very indistinct beginning that gradually increased in amplitude so that no sharp phases could be detected in the train of seismic signals. Precise locations could not be determined for these events, but they appeared to originate in the vicinity of the cavity. These emergent events were not studied in detail.

From the thousands of earthquakes that were recorded, 640 were selected for study. These events were chosen to delineate the zone of seismic acivity. To assure that all areas of activity were delineated, the records were systematically searched for earthquakes having an unusual set of relative arrival times. All but three of the 640 earthquakes located were within 13 km of ground zero (Fig. 1). Most of the epicenters lie in a north-trending zone, 15 km long and 3 km wide, passing about 3 km west of ground zero. The three events located outside the area shown in Fig. 1 may not be related to the Benham test (*11*).

The pattern of seismic activity shifted with time. In the first week, most of the earthquakes were within 7 km of ground zero; most of the earthquakes in the vicinity of the cavity occurred within this period. The activity west-southwest of ground zero showed a clear southward migration. During the third week several earthquakes of magnitude greater than 4.0 occurred in this zone, and the rate of occurrence of aftershocks increased dramatically along a 3- to 4-km southward extension of this north-south lineation.

There are two patterns of *P*-wave first motion. One pattern indicates strike-slip movement either in a right-lateral sense on a north-striking vertical plane or in a left-lateral sense on an east-striking vertical plane. The earthquakes exhibiting this pattern had epicenters in the north-trending lineation that passes approximately 4 km west of ground zero. It can be inferred that the nodal plane with the northerly strike corresponds to the fault plane and that right-lateral movement occurred along this north-south fault. The other pattern of *P*-wave first motion is associated with north-northeast-trending epicentral zones and indicates that the movement there was predominantly dip-slip. It should be emphasized that the areas of the strike-slip and dip-slip movement are distinct. Three earthquakes in the immediate vicinity of the cavity produced purely dilatational patterns, as would an implosive source.

The axis of tension at the earthquake focus, as inferred from the first-motion pattern, was approximately horizontal in the northwest to southeast direction for every earthquake examined. The pressure axis, on the other hand, varied from near vertical, the orientation leading to dip-slip faulting, to horizontal in the northeast to southwest direction, the orientation for the strike-slip movement.

The detonation point of the Benham explosion was in bedded zeolitized tuff overlain by ashflow tuffs, rhyolite, and other bedded tuffs. All of Pahute Mesa is underlain by such volcanic rocks, whose thickness at some places is greater than 4 km. The great thickness is due in part to filling of the Silent Canyon caldera, a circular collapse feature with a diameter of about 20 km. The caldera is about 13 million years old and is now buried by younger rocks (*12*).

North-trending faults are the most common structures exposed on the mesa (Fig. 2). They are more abundant in the older rocks, which are widely exposed in the eastern part of the mesa. The western part is generally covered by younger rocks and contains fewer exposed faults; there are undoubtedly faults covered by the younger rocks.

As expected, the Benham event caused movement on nearby faults for thousands of meters (Fig. 2). Faulting with a vertical displacement of as much as 0.3 m at the fault trace occurred along an 8.5-km segment of the north-trending fault that passes 2 km east of ground zero. A level line survey showed 0.76 m displacement across the fault in a zone 3 km wide. Another fault that branches to the northwest off the longest fault was fractured for 5.5 km with a maximum of 0.5 m vertical displacement. Both of these fault zones have right-lateral movement along them of about 30 cm as determined by a geodimeter survey. Two other fault zones, one 2700 m east and one 610 m west of ground zero, were fractured for an extent of 1200 and 1500 m, respectively. Less than 0.2 m vertical displacement occurred along these zones.

The great majority of aftershock epicenters occurred near a north-trending zone of small faults (Fig. 1) that cut the youngest volcanic rocks on the mesa. Accumulated vertical displacement along these faults before the explosion is only a few meters. Inspection while aftershocks were occurring showed a few fresh cracks with no significant displacement. Cracks occur discontinuously for about 1 km along the fault 4500 m due west of ground zero. The north-trending zone of small faults is believed to be the surface expression of a major fault zone buried by younger volcanic rocks. The epi-

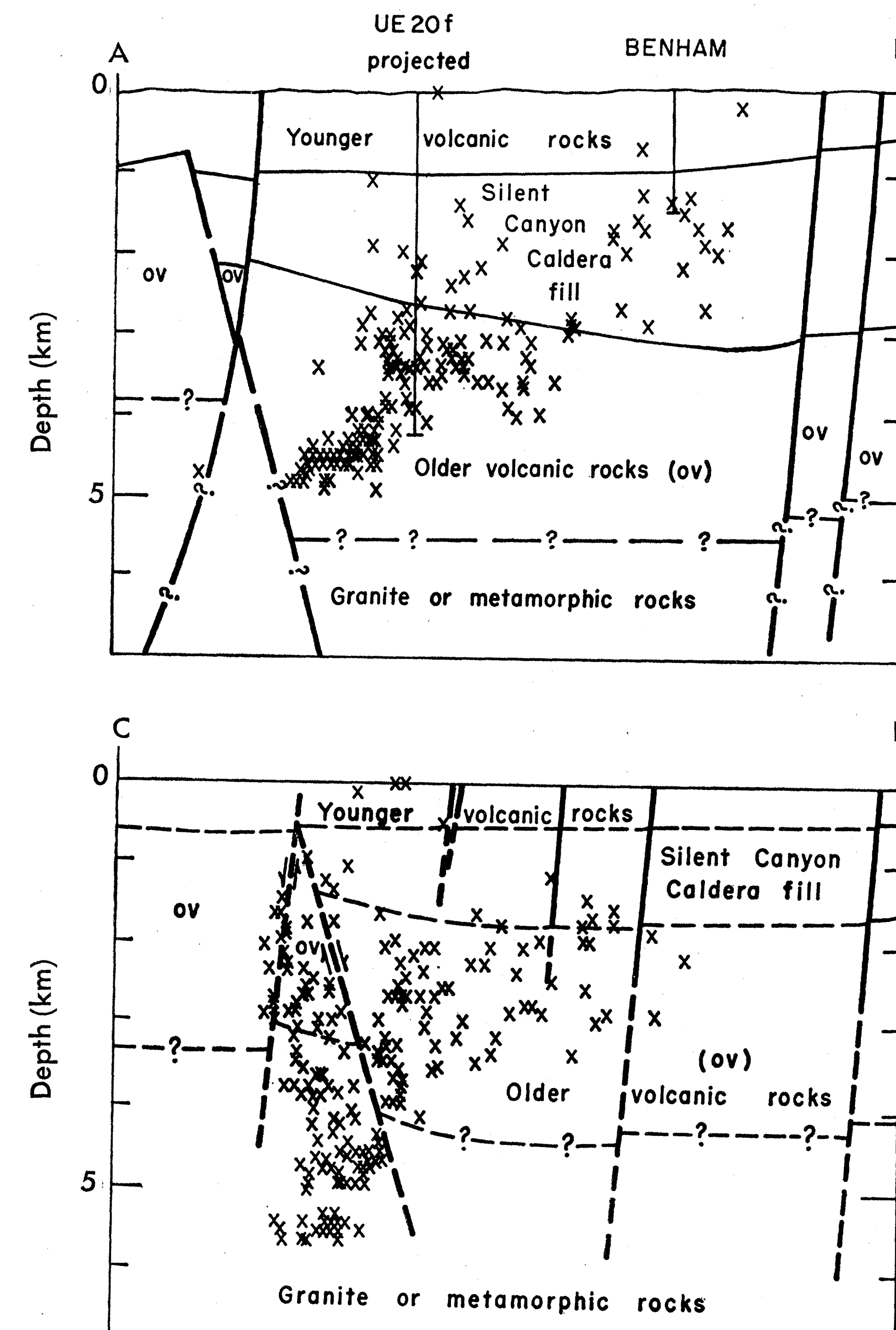

Fig. 2. Vertical sections (no vertical exaggeration) showing hypocenters (crosses) and generalized geology. Hypocenters projected lie within 1.23 km of plane *A-B* or within 2.45 km of plane *C-D*. Arrows along the faults indicate the sense of movement across the fault in the plane of the vertical section.

central zone, as well as the faults that had movement at the surface, can be interpreted as part of a basin-and-range fault system that extends under Pahute Mesa from the eastern side of Gold Flat, which is north of the mesa. Immediately south of Pahute Mesa, the fault system is obliterated by younger volcanic structures and rocks. The east-trending zone of epicenters 3.5 km south of ground zero nearly coincides with the exposed edge of the Timber Mountain caldera. These epicenters may have been controlled by the outermost ring fractures of the caldera.

Although some fracturing occurred within the zone of epicenters, the major movements were located to the east of it. Some understanding of this apparently rather puzzling relation can be gained by considering the distribution of the depth of the earthquakes together with the geologic structure (Fig. 2).

The focal depths of the earthquakes ranged from near zero to approximately 6 km. Most of the foci in the eastern part of the seismic region are in the depth range 1 to 4 km. In the western part the depths reach 6 km. Northwest of ground zero the seismic zone dips about 45°NW. This part of the seismic zone may correlate with the boundary of the Silent Canyon Caldera (*12*). Probably all hypocenters (Fig. 2) are within volcanic rocks despite the queried contact between older volcanic rocks and granite or metamorphic rocks. A drill hole (UE20f) 4170 m deep in the vicinity of these hypocenters bottomed in volcanic rock, and it is estimated that at least another 1000 m of volcanic rock occurs below the bottom of the hole (*13*). To the southwest, the zone is essentially vertical to a depth of 6 km. The earthquakes in this region may define the extension under the younger volcanic rocks of the north-trending fault that lies to the south (Fig. 1) and appears to lead into the seismic trend.

These findings suggest that the Benham explosion initiated movement along previously existing geologic boundaries. Movement at the surface occurred mainly along faults east of ground zero and was not associated with significant earthquake activity. West of the faulting, earthquakes occurred to about the depth of basement; farther west they define dipping zones that may correlate with similarly dipping basin-and-range structure. The tendency of some of the earthquakes to be aligned along parts of caldera boundaries and for nearly all of the earthquakes to be in volcanic rocks within a caldera seems to imply a genetic relationship. Additional information and study are required, however, to confirm the exact relationship.

We conclude that the seismic activity and the fault movement result primarily from the release of natural tectonic strain initiated by the explosion. The lack of radial symmetry in the distribution of epicenters, the pattern of *P*-wave first motions, and the correlation with preexisting geologic structures support this conclusion. In addition, the consistent northwest to southeast directions for the tension axes determined from the fault-plane solutions are in agreement with the direction of extension found for the earthquake near Fairview Peak in central Nevada (*14*) and with the extension direction indicated by the Raleigh wave radiation pattern produced by the Hardhat explosion in Yucca Flat at the Nevada Test Site (*7*).

R. M. HAMILTON
U.S. Geological Survey, Menlo Park, California 94025
F. A. MCKEOWN
U.S. Geological Survey, Denver, Colorado 80225
J. H. HEALY
U.S. Geological Survey, Menlo Park, California 94025

References and Notes

1. R. B. Hoy, *Bull. Seismol. Soc. Amer.* **53**, 845 (1963).
2. D. D. Dickey, F. A. McKeown, W. L. Ellis, *Technical Letter: Special Studies—65, U.S. Geol. Surv. Open File Report* (1968).
3. D. D. Dickey, E. C. Jenkins, F. A. McKeown, W. H. Lee, *Technical Letter: NTS-196, U.S. Geol. Surv. Open File Report* (1967); D. D. Dickey, *Geol. Soc. Amer. Mem.* **110**, 219 (1968); F. A. McKeown, D. D. Dickey, W. L. Ellis, *Technical Letter: Central Nevada-16, U.S. Geol. Surv. Open File Report* (1968).
4. W. H. Westphal, *Stanford Res. Inst. Final Rep. VUP-0607, Project 7.6* (1962); *Stanford Res. Inst. Tech. Rep. 6, Project 7.6* (1964).
5. F. Press and C. Archambeau, *J. Geophys. Res.* **67**, 337 (1962).
6. J. N. Brune and P. W. Pomeroy, *ibid.* **68**, 5005 (1963).
7. M. N. Toksöz, A. Ben-Menahem, D. G. Harkrider, *ibid.* **70**, 907 (1965).
8. G. Boucher, A. Ryall, A. E. Jones, *ibid.* **74**, 3808 (1969).
9. J. F. Evernden, *Trans. Amer. Geophys. Union* **50**, 247 (1969).
10. A. Ryall and W. U. Savage, *J. Geophys. Res.* **74**, 4281 (1969).
11. One of the earthquakes beyond 13 km was located 22 km northwest of ground zero and the other two were 21 km southeast. All three earthquakes occurred during the second week after the explosion.
12. P. P. Orkild, F. M. Byers, Jr., D. L. Hoover, K. A. Sargent, *Geol. Soc. Amer. Mem.* **110**, 77 (1968).
13. P. P. Orkild, personal communication.
14. L. J. Meister, R. O. Burford, G. A. Thompson, R. L. Kovach, *J. Geophys. Res.* **73**, 5981 (1968).
15. Mapping aspects supported by U.S. Atomic Energy Commission.

20 August 1969

Freshwater Ferromanganese Concretions: Chemistry and Internal Structure

Abstract. *Studies by optical microscopy, x-ray diffraction, and electron probe techniques of ferromanganese concretions from three Canadian lakes reveal chemical banding of amorphous hydrated iron and manganese oxides. The average ratio of iron to manganese in concretions from these lakes varies from 0.43 to 2.56. The concentrations of cobalt, nickel, copper, and lead are one to two orders of magnitude below those reported for oceanic ferromanganese concretions.*

Freshwater ferromanganese concretions have been observed in small lakes in eastern Canada, Scandinavia, western Russia, northern England, and New England, and in the Great Lakes (*1–3*). Thus far there have been no reported occurrences of ferromanganese concretions in freshwater environments in subtropical or tropical regions. This report presents the results of the first detailed study on the mineralogy, internal structure, and chemistry of freshwater ferromanganese concretions from Canadian lakes.

The presence of ferromanganese concretions in Canadian lakes has been reported by Honeyman (*4*) and by Kindle (*5*). Concretions for this study were collected from Grand Lake and Ship Harbour Lake, Nova Scotia, and Mosque Lake, Ontario. The geological environment of these lakes is very different, with the Nova Scotia lakes being developed on sedimentary rocks of different ages and the Ontario lake overlying biotitic gneisses. All of the concretions discussed here were collected in 0.5 to 2.0 m of water. The substrate at all the concretion sites visited consisted of coarse-grained quartz sand and pebbles. The ferromanganese precipitate forms on a pebble nucleus and always exhibits a maximum thickness in a zone 0.5 to 3.0 cm above the sediment-water interface. The nuclei for concretion formation include slate, sandstone, and granite pebbles. No particular type of rock seems to be preferred for nucleation. The morphology of ferromanganese concretions in Canadian lakes varies from bands of precipitate which grow parallel to the sediment-water interface to nodular concretions where ferromanganese oxide completely encloses the rock nucleus.

Examination of the ferromanganese precipitate by optical, x-ray diffraction,